USGS Award No. 04HQGR0072

USING HIGH-RESOLUTION SATELLITE IMAGERY TO PROVIDE RAPID POST-EARTHQUAKE DAMAGE DETECTION

Ellen M. Rathje, Ph.D., P.E.
University of Texas at Austin
ECJ 9.227, C1792
Austin, TX 78712
Tel: 512-471-4929
Fax: 512-471-6548
e.rathje@mail.utexas.edu
http://www.ce.utexas.edu/dept/area/geotech/GeotechnicalEngr.htm

Melba M. Crawford, Ph.D.
Purdue University
LARS: Lilly Hall
915 W. State St.
West Lafayette, IN 47907-2054
Tel: 765 496-9355
Fax: 765 496-2926
mcrawford@purdue.edu

NEHRP Element: II
Key Words: Earthquake Damage, Remote Sensing, Satellite Imagery

Research supported by the U.S. Geological Survey (USGS), Department of the Interior, under USGS award number (04HQGR0072). The views and conclusions contained in this document are those of the authors and should not be interpreted as necessarily representing the official policies, either expressed or implied, of the U.S. Government

ABSTRACT

The objective of this research is to investigate the use of high-resolution optical satellite imagery to develop estimates of earthquake damage patterns in urban areas. Pre- and post-earthquake satellite images (0.6 m resolution) from the 26 December 2003 Bam, Iran earthquake were used to investigate damage patterns within the city of Bam, Iran. The post-earthquake image was used alone in a thematic classification algorithm to identify pixels that represent earthquake damage, while the pre- and post-earthquakes images were used together in a change detection algorithm to identify changed pixels that presumably were changed due to damage from the earthquake. For both sets of analyses, the damage information on the pixel scale was used to define damage intensities across the city. Damage intensity was defined as the percentage of pixels within a 60 m by 60 m area identified as damage. The resulting damage intensities were compared with damage results from field surveys.

Damage patterns from both remote sensing techniques (thematic classification, change detection) generally agreed with damage patterns from field surveys, although the remote sensing results provided information at a smaller spatial scale. Thematic classification appeared to overestimate some damage due to misclassification of pixels, while change detection overestimated damage in some areas due to the presence of non-earthquake change. On-going research is focusing on developing a multi-resolution approach that integrates content dependent texture measures and using object-oriented classification that classifies objects rather than pixels. The objective of this work is to increase sensitivity while keeping the false detection rate low.

NON-TECHNICAL SUMMARY

With the successful launch of high-resolution commercial satellites, the ability to identify earthquake-induced damage from satellite imagery is a reality. These commercial satellites collect digital data at spatial resolutions as high as 0.6 m, and therefore contain a wealth of information for mapping earthquake damage. Several methodologies developed in image and signal processing for thematic mapping and monitoring change in multi-temporal data sets can be utilized to extract this information. This study shows that image processing techniques applied to high resolution satellite imagery can be used to develop detailed damage maps of urban areas after earthquakes.

INTRODUCTION

High-resolution (0.6 m) commercial satellite images contain a wealth of information for mapping earthquake damage. Several methodologies developed in image and signal processing for thematic mapping and monitoring change in multi-temporal data sets can be utilized to extract this information. This study used pre- and post-earthquake satellite images from the 26 December 2003 Bam (M_w = 6.6) earthquake to identify earthquake damage in the city of Bam. Bam is a city of approximately 90,000 residents (200,000 people live in the greater Bam area) located less than 10 km from the earthquake. Pre- and post-earthquake satellite images of Bam were acquired by the Quickbird satellite (www.digitalglobe.com) on 30 September 2003 and 3 January 2004, respectively. Visual comparison of the pre- and post-earthquake images provided information about the characteristics of damage within the city. To develop detailed information regarding damage patterns across the city, semi-automated thematic classification methods were applied solely to the post-earthquake image and a change detection algorithm was applied to the pre- and post-earthquake images. The results from the pixel-based thematic classification and change detections analyses were used to define the damage intensity (DI) within 60 m by 60 m areas. These results were compared with field surveys of damage from Bam.

DAMAGE CHARACTERISTICS

The pan-sharpened satellite image of central Bam acquired after the earthquake on 3 January 2004 is displayed in Figure 1. The layout of the city is clearly discernable, with roads, vegetation, buildings easily identified. The central and western sections of the city are characterized by large vegetated areas, while the eastern section of the city has the highest population density.

Figure 2 shows pre- and post-earthquake images of areas within the city with different degrees of damage. An area with moderate damage is shown in Figures 2(a) and (b). The pre-earthquake image (Figure 2(a)) contains small, adobe structures along the streets throughout this area. In the post-earthquake image (Figure 2(b)), the streets and most of the buildings are still apparent, but several of the structures at the bottom of the image are destroyed. An area of almost complete destruction is shown in Figures 2(c) and (d). Again, the roads and structures are easily visible in the pre-earthquake image (Figure 2(c)). However, it is hard to distinguish roads or structures in the post-earthquake image (Figure 2(d)) because of the intense damage. This dramatic change in image pattern is characteristic of earthquake damage, particularly for adobe-type structures. These types of structures tend to completely crumble during an earthquake, leaving little indication of the shape or form of the original structure. For engineered structures (e.g., reinforced concrete frame buildings), the image characteristics of damage are somewhat different, as these structures tend to pancake and maintain some of the shape and form of the original building (Rathje and Crawford 2004).

Figure 3 shows pre- and post-earthquake images of the Arge-Bam Citadel which is located in the northern section of Bam (see upper right corner of Figure 1). This Citadel has survived in Bam for over 2000 years, but was severely damaged during the earthquake. The pre-earthquake image (Figure 3(a)) of the Citadel compound clearly shows a large complex of smaller buildings surrounded by a series of walls. In the post-earthquake image (Figure 3(b)), the edges of the smaller buildings are missing, indicating their collapse. Field investigations

reported that 80% of the buildings in the Citadel complex experienced complete collapse (EERI 2004). This report is consistent with the observations from the satellite images.

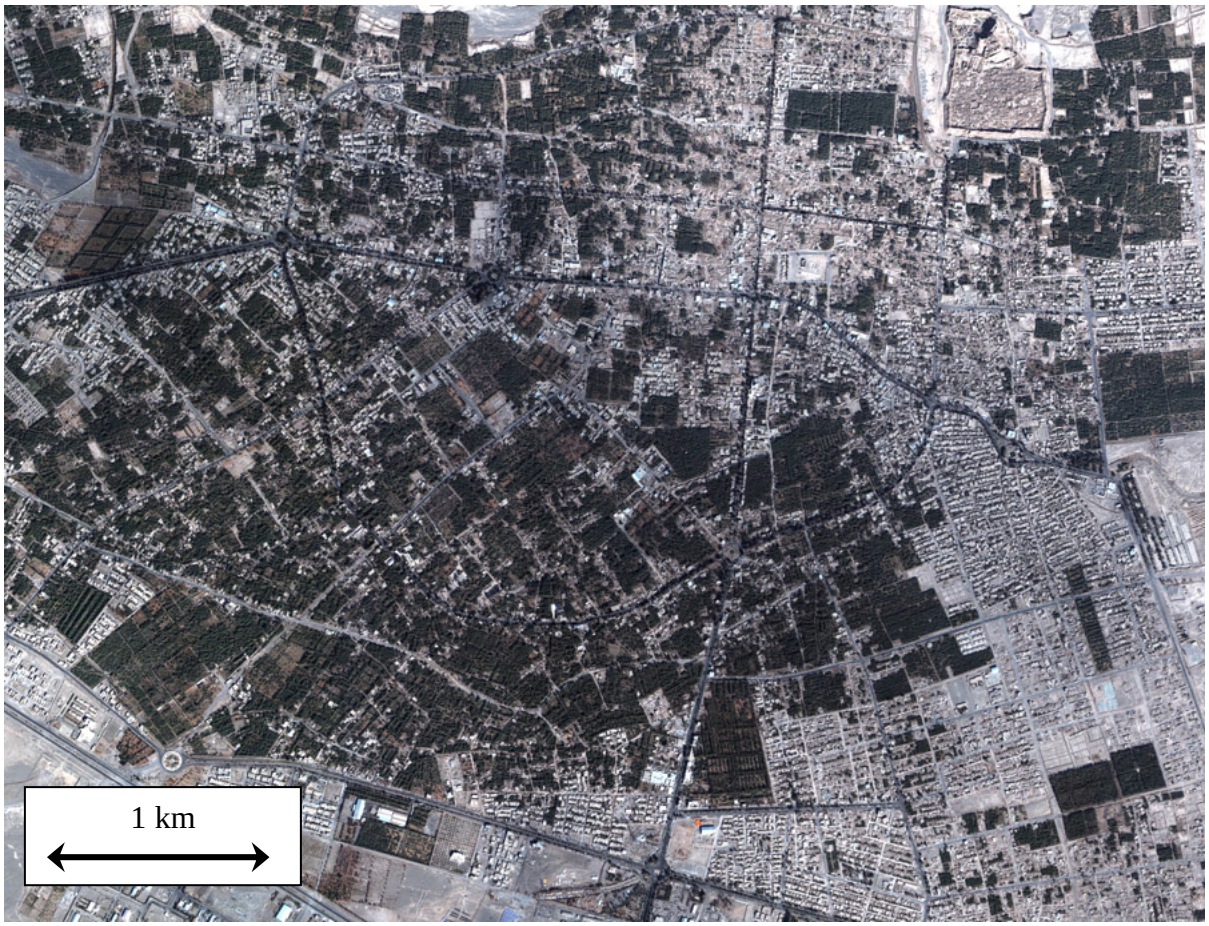

Figure 1. Satellite image of central Bam acquired after the earthquake on 3 January 2004 (image courtesy of DigitalGlobe).

Figure 2. (a) Pre-earthquake and (b) post-earthquake image in moderately damaged area; (c) pre-earthquake and (b) post-earthquake image in heavily damaged area (images courtesy of DigitalGlobe).

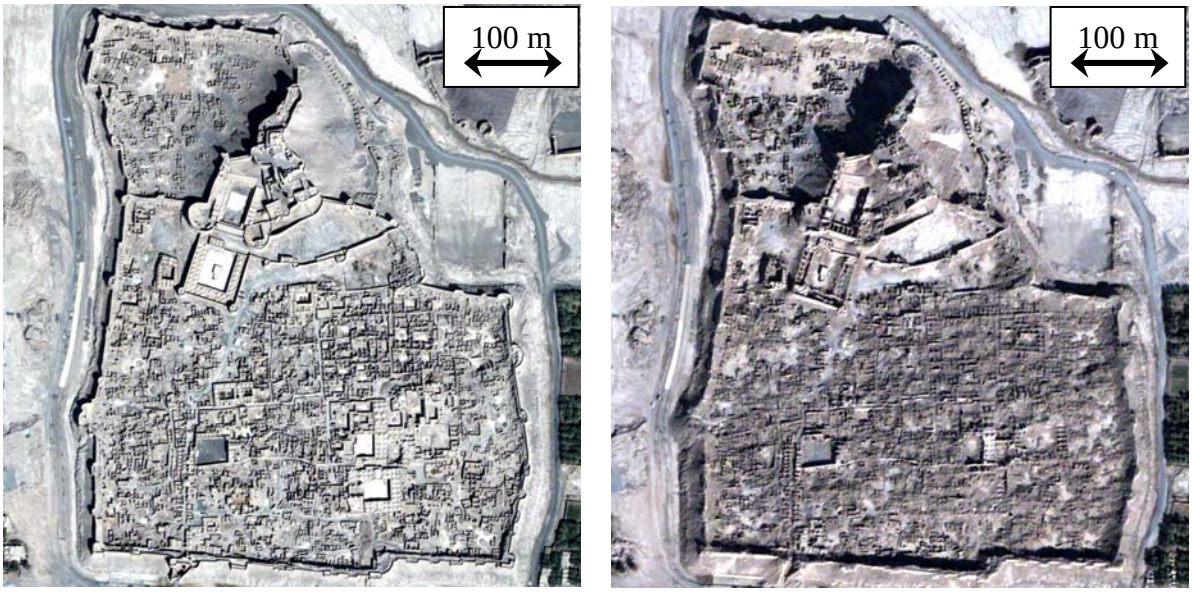

Figure 3. (a) Pre-earthquake and (b) post-earthquake image of the Arge-Bam Citadel in Bam (images courtesy of DigitalGlobe).

ANALYTICAL TECHNIQUES FOR IDENTIFYING EARTHQUAKE DAMAGE

Thematic classification is commonly used to analyze remotely sensing data and involves classification of individual pixels based on the values of the features associated with that pixel. As previously discussed, thematic classification of optical satellite data is often used to identify land use and land cover classes, but it can also be used to identify urban damage after an earthquake. Earthquake damage detection using thematic classification involves identifying the classes within an urban setting (e.g., undamaged buildings, damaged buildings, roads, vegetation, etc) and assigning each pixel to one of these classes. Supervised classification techniques utilize training data (pixels in which their classes are known) to train the classification algorithm, such that the remaining pixels are placed within one of the classes based on a statistical comparison with the training data. One of the most commonly used supervised classification algorithms is the maximum likelihood (ML) method whereby the parameters of the probability density function for each class are estimated from the training data, and each unlabeled pixel is assigned to a relevant class based on the highest value of the likelihood function. Thematic classification is an attractive approach for earthquake damage detection because it requires only a post-earthquake image. However, a critical part of the classification process is the choice of the characteristics that distinguish the various classes.

Digital optical satellite data represent the spectral responses within each of the spectral bands. However, the digital data (DN values) also can be used to derive additional image characteristics for use in subsequent analysis. Image texture and edge density are two classes of characteristics that are often used in image processing. Texture measures provide information about the spatial distribution of variations in pixel intensity in an image (Haralick et al. 1973). Texture tends to be a stable parameter that does not change significantly with season or illumination, unlike spectral characteristics that often change with the seasons as vegetation and sun angles change. Traditional quantitative textural measures consider the change in gray scale

across an image area using statistical measures. Julesz (1975) indicates that second-order statistics derived from the gray-level co-occurrence matrix (CM) of an image often provide the most useful information regarding texture. The values of CM(i,j) are the probabilities (p(i,j)) that a pair of DN levels (i,j) within a window occur at a separation distance of (x,y). To compute the CM, a window size and a separation distance must be defined. Each pixel (reference pixel) within the window then is compared with the pixel located a distance (x,y) from the reference pixel (the neighbor pixel). If an area has "smooth" texture, reference and neighbor pixels will tend to have similar DN values (i.e., $i \sim j$). A large number of similar DN values result in large values close to the diagonal of the CM and small values away from the diagonal. If an image has "rough" texture, reference and neighbor pixels will tend to have dissimilar values of DN (i.e., $i >> j$ or $i << j$), which results in more scatter about the diagonal within the CM. Haralick et al. (1973) proposed a variety of scalar texture measures that are based on the scatter with the CM. The spatial distribution of edges also may play a role in identifying various characteristics within a satellite image (e.g., buildings). In an image, edges represent areas that have a rapid change in intensity. For example, the edge of a building is represented by a rapid change from the color of the building roof to the color of the surrounding area. There are several methodologies available to identify edges in digital images. One of the most robust methods is the Canny edge detection algorithm (Canny 1986) because it often captures the most edges in the most detail and it minimizes false detections (Bowyer et al. 1999). After identifying edge pixels using the Canny edge detector, the edge density can be defined as the percentage of edges within a specified window.

Change detection is the process of identifying pixels that have changed between two images obtained at different times. Change detection is an attractive approach for earthquake damage detection because it involves identification of major changes between pre- and post-earthquake images. However, this approach requires that a pre-earthquake image of the area be available in the commercial image archive, which is not always the case. Some frequently used change detection methods include image differencing, image ratioing, and image-to-image correlation (Singh 1989). Image differencing and ratioing involve simply computing the difference or ratio between pixel values in the two images, while image-to-image correlation involves computing the sample correlation coefficient within small windows between the two images. The sample correlation coefficient for a windowed area is given by:

$$r = \frac{n\sum PV_a PV_b - \left(\sum PV_a\right)\left(\sum PV_b\right)}{\sqrt{n\sum PV_a{}^2 - \left(\sum PV_a\right)^2} \cdot \sqrt{n\sum PV_b{}^2 - \left(\sum PV_b\right)^2}} \qquad (1)$$

where PV_a is the pixel value in the pre- earthquake image, PV_b is the corresponding pixel value in the post earthquake image, n is the number of pixels in the correlation window, and the summation is performed over all pixels in the window. As with thematic classification, the features that will be used in the change detection analysis must be selected, and a threshold must be chosen that identifies significant change.

DAMAGE IDENTIFICATION RESULTS

Earthquake damage assessment via thematic classification uses only the post-earthquake imagery. Six classes were visually selected for the city of Bam: (1) damaged areas, (2) undamaged buildings, (3) vegetation, (4) open ground, (5) shadow, and (6) asphalt roads.

Thirty-one features initially were considered for the ML classification; the four spectral bands, eight texture measures based on the elements of the CM and computed for three window sizes and horizontal separation distances, and edge density computed for the same three window sizes. The eight texture measures were based on the work of Haralick et al. (1973): contrast = CON = $\Sigma (i - j)^2 \, p(i,j)$, dissimilarity = DIS = $\sum | i - j | \cdot p(i,j)$, homogeneity = HOM = $\Sigma \, p(i,j) / [1 + (i - j)^2]$, angular second moment = ASM = $\Sigma \, p(i,j)^2$, entropy = ENT = $-\Sigma \, p(i,j) \log p(i,j)$, mean = MEAN = $\Sigma \, i \cdot p(i,j)$, variance = VAR = $\Sigma \, (i - \text{MEAN})^2 \cdot p(i,j)$, and correlation = COR = $\Sigma \, (i - \text{MEAN}) \cdot (j - \text{MEAN}) \cdot p(i,j) / \text{VAR}$. The three window sizes (used for both the texture and edge calculations) and separation distances were: a 6 by 6 pixel window with a 3 pixel horizontal separation distance, a 10 by 10 window with a 5 pixel separation, and a 25 by 25 window with a 12 pixel separation. Investigation of the contribution of the features to separating the classes (Woo et al. 2005, Rathje et al. 2005b) reduced this number to fourteen (blue, green, red, near infrared, MEAN6/3, ENT6/3, COR6/3, MEAN10/5, CON10/5, ENT10/5, ASM10/5, COR10/5, CON25/12, and COR25/12). The result of the ML classification is shown in Figure 4. Damage (shown in red) is concentrated in the eastern sections of the city, which is consistent with damage observations from the field (Nazem 2003). However, damage pixels are also scattered throughout the city; in some instances these areas represent smaller pockets of damage, while in other instances they represent bare areas whose features are similar to damaged areas and, thus, were misclassified. The most undamaged buildings (shown in blue) are found along the eastern and southern edges of the city, and the center of the city mostly consists of vegetated areas.

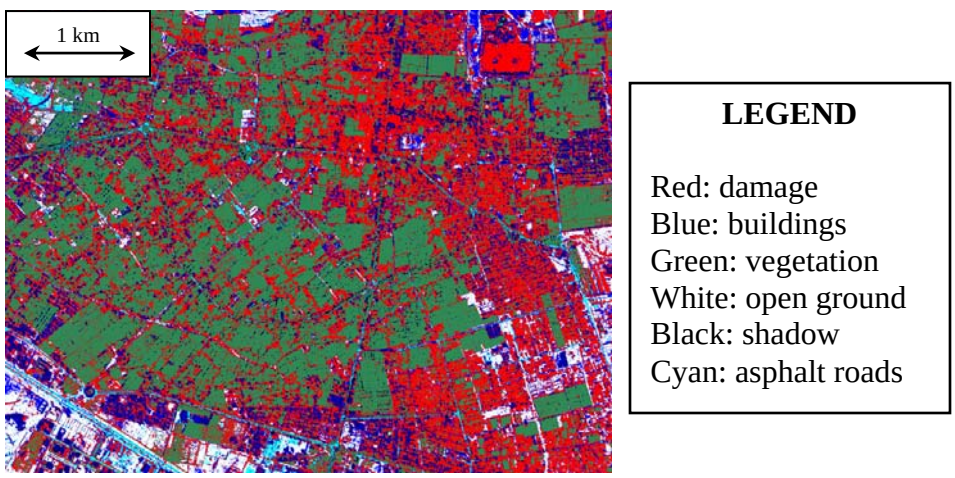

Figure 4. Results of ML classification of post-earthquake image of Bam.

The change detection algorithm utilized in this study is based on the sample correlation coefficient (equation 1) computed for the co-registered, pre-earthquake and post-earthquake image data. Changes in texture were found to be most useful in identifying earthquake damage, and for this analysis the textural feature VAR31/15 was used and a 15 by 15 pixel window was employed to compute the sample correlation coefficient (Rathje et al. 2005a). Through comparisons of the histograms of r computed for damaged and undamaged areas of the city, a threshold of 0.5 (i.e., $r < 0.5$ indicates earthquake damage) was selected (Rathje et al. 2005a). Finally, because some image change is associated with vegetation and shadow due to variations in sun angle, seasons, etc., between image acquisitions, a mask that removes vegetation and shadow pixels from the changed pixels was applied. The damaged areas identified by change

detection are shown in red and superimposed on the post-earthquake satellite image in Figure 5. Similar to the ML classification, the change detection results indicate a concentration of damage in the eastern part of the city, although the damage appears to be most continuous in the north-east corner and the south-east corner of the image.

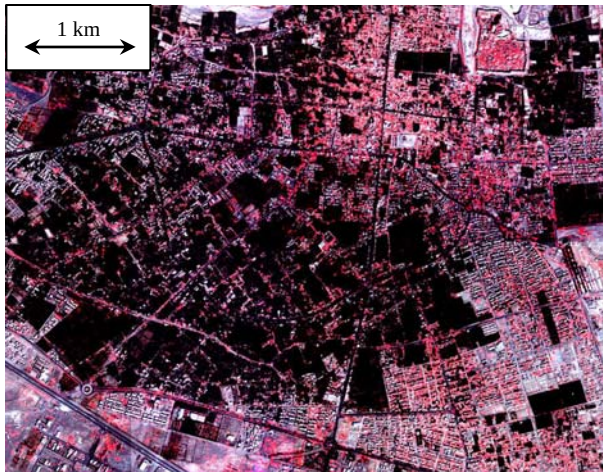

Figure 5. Earthquake damage (shown in red) for the city of Bam identified by change detection.

The thematic classification and change detection results both indicate concentrations of damage in the eastern sections of Bam. However, it is difficult to quantify damage information from the analytical results as presented in Figure 4 and 5. To provide a more quantitative assessment of earthquake damage and to provide an easier means to quantitatively compare the results from thematic classification and change detection, a damage intensity measure was defined. The identified damaged pixels are used to compute the damage intensity (DI), which is defined on the percentage of pixels within a 100 by 100 pixel (60 m x 60 m) window. The DI scale was defined as DI5 = 80-100% damage, DI4 = 60-80% damage, and DI3 = 40-60% damage. DI less than 40% was not considered significant based on visual examination of the damage in areas with DI < 40%, and this observation indicates that there is some misidentification of damage in the analyses.

The resulting damage intensities from the ML classification and the change detection analysis are shown in Figure 6, overlain on the Quickbird images. The DI3 regions are marked as green, the DI4 regions as blue, and the DI5) regions as red. This representation of the damage assessment again indicates intense damage in the eastern part of the city, with significant areas labeled as DI4 and DI5. However, a detailed examination of the distribution of DI within the city reveals differences between the ML classification and change detection analysis. The ML classification identified a larger total area of damage, with 38% of the image identified as DI3, DI4, or DI5, as opposed to 24% from change detection. In terms of the distribution of DI, the ML classification identified 5.16 km^2 of DI3, 2.63 km^2 of DI4, and 0.44 km^2 of DI5, while change detection identified 2.98 km^2 of DI3, 1.79 km^2 of DI4, and 0.48 km^2 of DI5. Thus, the biggest difference occurs between the identification of DI3 and DI4, which is apparent in Figure 6 with significantly more D3 (green) areas from the ML classification. Additionally, Figure 6(c) shows damage patterns in Bam as assessed by field surveys (Nazem 2003). The field survey used a damage intensity scale based on the percentage of buildings destroyed, with purple areas having 80-100% buildings destroyed (high damage – HD), red areas having 50-80% destroyed

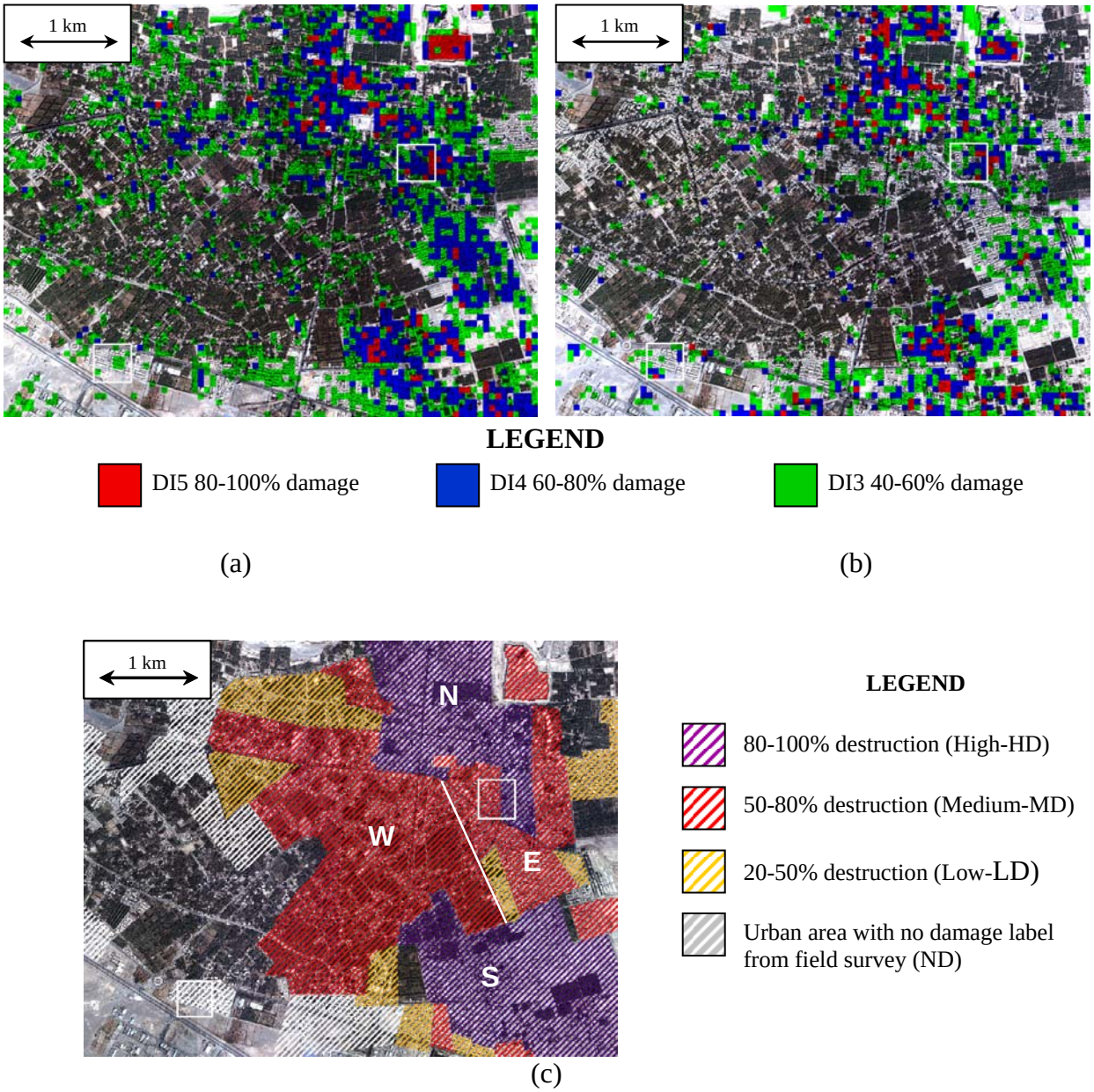

Figure 6. Damage Intensity (DI) results from (a) maximum-likelihood classification and (b) change detection analysis. (c) Results from field damage survey (after Nazem 2003).

(medium damage – MD), and yellow areas having 20-50% destroyed (low damage – LD). However, it is unclear exactly how the field damage data were collected and interpreted. Nonetheless, the field survey data indicate two pockets of heavy damage: one in the northeast and one in the southeast of the city. Considering DI4 (blue) and DI5 (red) areas from the remote sensing results (Figures 6(a) and (b)), the change detection results more closely match this observation from the field results. The ML classification results show large zone of D4 throughout the entire eastern part of the city, rather than the two pockets of heavy damage

identified from the field survey (purple areas) or the change detection result (Figure 6(b)). Nonetheless, the remote sensing results (both ML and change detection) provide a more detailed assessment of damage distribution across the urban infrastructure. Rather than assigning damage assessments over broad areas or regions (> 1 km^2) of a city, the remote sensing approach can delineate and distinguish damage over a much smaller area.

Two areas within the city were isolated for a closer comparison between the damage results, and these areas are indicated in Figure 6 and shown in Figures 7 and 8. Figure 7 represents a non-damaged area (see Figure 6(c)) within southwest Bam, and the pre- and post-earthquake images of this area and the damage intensity results from the two methodologies are shown. The results from the ML classification (Figure 6(c)) indicate some small areas of damage, although no damage can be visually identified in the image (Figure 7(b)). These small areas of damage are caused by misclassification of pixels during the classification process. The change detection results (Figure 7(d)), reveal some areas of heavy damage (DI4 and DI5), mostly because of non-earthquake change observed in the image. In particular, the eastern and southwestern parts of the area experienced change due to the presence of vehicles on roads and open ground. Because change detection analysis assumes all change is earthquake related, the earthquake damage assessment in this area is overestimated. This result shows that, although the developed change detection algorithm removes non-earthquake changes associated with vegetation and shadow, the identification of other sources of non-earthquake change is one shortcoming of using change detection to evaluate earthquake damage patterns.

Figure 8 represents an urban area in eastern Bam (Figure 6) that was heavily damaged after the earthquake. Based on visual examination of the post-earthquake image in Figure 8(b) and the field survey results in Figure 8(e), the destruction in this area is more severe east of the north-south road, but less severe to the west of the road. The maximum-likelihood classification (Figure 8(c)) identifies DI4 damage across most of the image, with a concentration of DI5 along the eastern edge. Although the DI5 areas correspond with the heaviest damage within the image, some of the DI4 areas correspond with areas that are not severely damaged. This discrepancy is caused by confusion within the classification algorithm that incorrectly identifies some areas as damage. The results from change detection (Figure 8(d)) identify DI4 and DI5 areas east of the road and DI3 and non-damaged areas west of the road. This assessment of damage is in better agreement with the visual assessment of damage in the area, indicating that change detection can better distinguish between different intensities of severe damage.

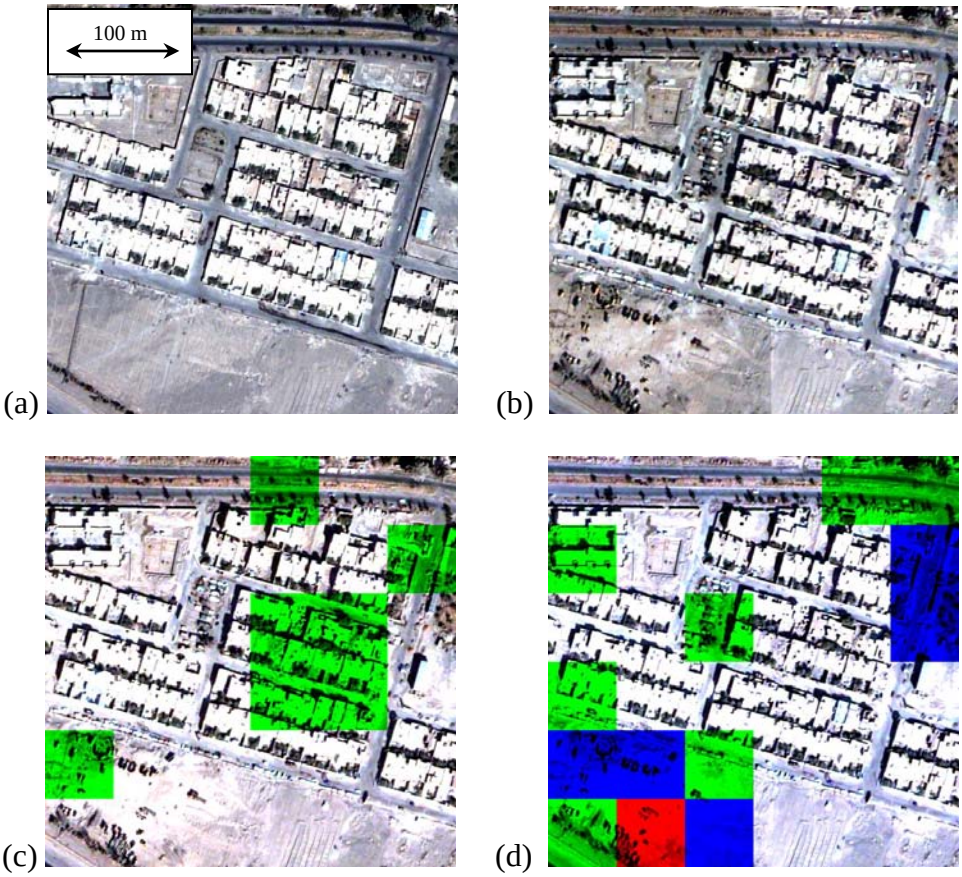

Figure 7. (a) Pre-earthquake and (b) post-earthquake image within southwestern Bam, and Damage Intensity results from (c) maximum-likelihood classification and (d) change detection.

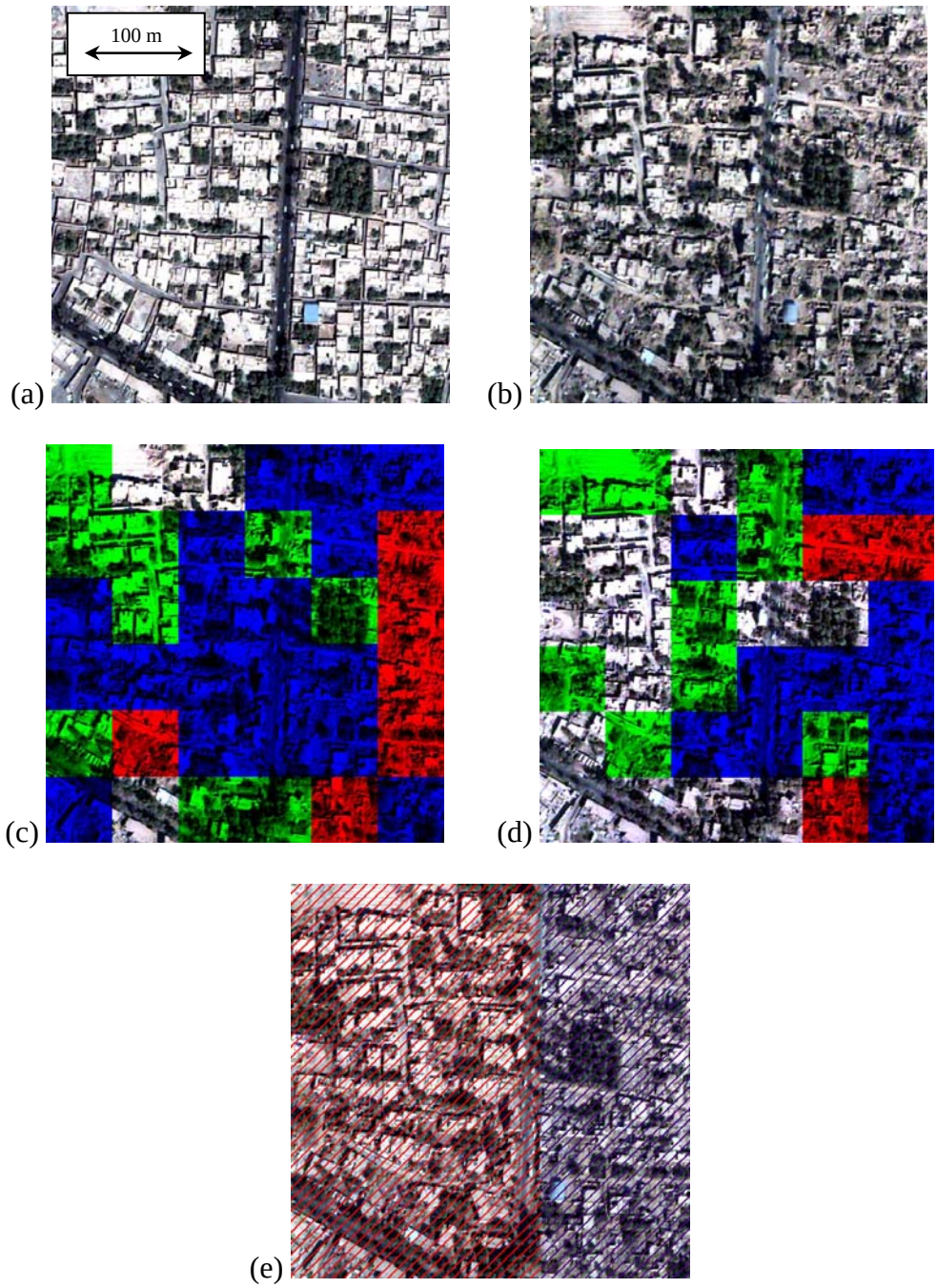

Figure 8. (a) Pre-earthquake and (b) post-earthquake image within eastern Bam, Damage Intensity results from (c) maximum-likelihood classification and (d) change detection, and (e) field survey results overlain on post-earthquake image (see Figure 6 for legend).

CONCLUSIONS

Currently, high-resolution optical satellites can be used to develop detailed damage assessments after natural disasters, such as earthquakes and hurricanes. Thematic classification, which utilizes only a pre-event image, and change detection, which uses both a pre- and post-event image, can be used to identify significant damage induced by natural disasters. Thematic classification and change detection algorithms for identifying urban earthquake damage were developed and applied to high-resolution optical satellite imagery obtained from the 2003 Bam, Iran earthquake. Damage patterns from both techniques generally agreed with damage patterns from field surveys, although the remote sensing results provided information at a smaller spatial scale. Thematic classification appeared to overestimate some damage due to misclassification of pixels, while change detection overestimated damage in some areas due to the presence of non-earthquake change. On-going research is focusing on developing a multi-resolution approach that integrates content dependent texture measures and using object-oriented classification that classifies objects rather than pixels. The objective of this work is to increase sensitivity while keeping the false detection rate low. Finally, the development of remote sensing-based earthquake damage assessments will be useful in providing rapid evaluations of human impact, estimating economic losses, and correlating damage patterns with soil conditions.

REFERENCES

Bowyer, K., Kranenburg, C., and Dougherty, S., (1999) "Edge detector evaluation using empirical ROC curves," *IEEE Computer Society Conference on Computer Vision and Pattern Recognition*, Vol. 1, 354-359.

Canny, J., (1986) "A Computational Approach to Edge Detection," *IEEE Transactions on Pattern Analysis and Machine Intelligence*, 8(6), pp. 679-698.

Earthquake Engineering Research Institute (EERI) "Preliminary Observations on the Bam, Iran, Earthquake of December 26, 2003" *EERI Newsletter*, April 2004.

Haralick, R.M., Shanmugan, K., and Dinstein, I. (1973) "Texture Features for Image Classification." *IEEE Transactions on Systems, Man, and Cybernetics*, SMC-3, pp. 610-621.

Julesz, B. (1975) "Experiments in the Visual Perception of Texture," *Scientific American*, 232, pp. 34-43.

Nazem Zade Shoaii, M., (2003) *Observation Report on the 26/12/2003 Earthquake of Bam, Southeast of Iran* (in Farsi), Geological Survey of Iran.

Rathje, E.M., and Crawford, M. 2004. "Using High Resolution Satellite Imagery to Detect Damage from the 2003 Northern Algeria Earthquake," Paper No. 2911, *13th World Conference on Earthquake Engineering*, Vancouver, Canada, August.

Rathje, E.M., Woo, K., Crawford, M., and Neuenschwander, A. (2005a) "Earthquake Damage Identification using Multi-Temporal High-Resolution Optical Satellite Imagery," *International Geoscience and Remote Sensing Symposium*, IEEE, Seoul, South Korea, July (CD-ROM).

Rathje, E.M., Crawford, M., Woo, K., and Neuenschwander, A. (2005b) "Damage Patterns from Satellite Images from the 2003 Bam, Iran Earthquake," *Earthquake Spectra*, Earthquake Engineering Research Institute, 21(S1), S295-307.

Singh, A. (1989) "Review Article: Digital Change Detection Techniques Using Remotely Sensed Data," *International Journal of Remote Sensing*, 10(6), pp. 989-1003.

Woo, K.-W., Rathje, E.M. and Crawford, M. (2005) "Comparison of Earthquake Damage Evaluation using Change Detection and Thematic Classification," *Workshop on Application of Remote Sensing Technologies for Disaster Response*, Chiba University, Chiba, Japan, 12-13 September.

PUBLICATIONS RESULTING FROM THIS WORK

Rathje, E.M., Woo, K.-W., and Crawford, M. 2006. "Spaceborne and Airborne Remote Sensing for Geotechnical Applications," Invited Paper, Proceedings, *GeoCongress'06 Geotechnical Engineering in the Information Technology Age*, February (CD-ROM).

Rathje, E.M., Crawford, M., Woo, K., and Neuenschwander, A. 2005. "Damage Patterns from Satellite Images from the 2003 Bam, Iran Earthquake," *Earthquake Spectra*, Earthquake Engineering Research Institute, 21(S1), S295-307.

Rathje, E.M., Woo, K., Crawford, M., and Neuenschwander, A. 2005. "Earthquake Damage Identification using Multi-Temporal High-Resolution Optical Satellite Imagery," *International Geoscience and Remote Sensing Symposium*, IEEE, Seoul, South Korea, July (CD-ROM).

Woo, K.-W., Rathje, E.M. and Crawford, M. 2005. "Comparison of Earthquake Damage Evaluation using Change Detection and Thematic Classification," *Workshop on Application of Remote Sensing Technologies for Disaster Response*, Chiba University, Chiba, Japan, 12-13 September.